Sensors & Actuators: A. Physical 348 (2022) 114018

Contents lists available at ScienceDirect

Sensors and Actuators: A. Physical

journal homepage: www.journals.elsevier.com/sensors-and-actuators-a-physical

Spherical probe for the thermophysical characterization of regoliths for planetary exploration using frequency methods

M. Domínguez-Pumar [a,*], C. Rosero-Pozo [a], J. Pons-Nin [a], J. Ramos-Castro [a], D. Szewczyk [b], A. Jeżowski [b], N. Solà-Peñafiel [a], X. Manyosa [a], S. Bermejo [a], V. Jiménez [a]

[a] Micro and Nano Technologies Group, Electronic Eng. Dept., Universitat Politècnica de Catalunya, Barcelona, Spain
[b] Institute of Low Temperature and Structure Research, Polish Academy of Sciences, Poland

ARTICLE INFO

Keywords:
Frequency methods
Regolith
Thermophysical properties

ABSTRACT

The objective of this paper is to analyse the capability of a spherical thermoprobe, recently proposed as a 3D heat flux sensor for regoliths, and additionally to characterize the thermophysical properties of regoliths. The sensor is based on the spherical structure of a Mars wind sensor. The characterization is carried out using frequency methods. Extensive experimental results have been obtained with eight regolith simulants made of glass microbeads. Errors in thermal conductivity and diffusivity are smaller than ± 7%, for these simulants.

1. Introduction

The characterization of the thermophysical properties of regoliths is one key measurement in planetary exploration [1–4]. This characterization can be made in situ, typically using an insertion mechanism or drilling [5,6], which can sometimes be complex [7]. Additionally, remote characterization is also possible through, for example, the interpretation of thermal inertia data [8]. Recently a 3D heat flux sensor has been proposed for thermal property determinations for regoliths [9]. The sensor is based on the spherical structure of a Mars wind sensor [10,11]. The objective of this study is to analyse the capability of this 3D heat flux sensor to additionally characterize the thermophysical properties of the regolith (thermal conductivity and diffusivity).

In order to characterize the thermal properties of the regolith frequency methods will be used. These methods are based on the interpretation of thermal impedances in the frequency domain of, typically, Pt resistors. It is possible to obtain dynamical models related to the sensor geometry [12,13]. One of the main advantages of frequency methods, compared to static measurements, is that a reference temperature for the regolith is not needed since the impedance measurements are obtained only from the amplitude and phase of the temperature/-power signals, or indirectly, from the electrical impedance of Pt resistors in the frequency domain.

The objective of this paper is therefore to show that the thermophysical properties of the regolith may be characterised using the spherical geometry of the thermoprobe. Experiments are presented in which thermal properties of eight different regolith simulants, made of hollow glass spheres, are characterized. The inferred thermal conductivity and diffusivity values are compared against reference values obtained in the laboratory using a KD2 Pro Thermal Properties Analyzer from Decagon Devices, Inc.

2. Sensor description

The thermoprobe is a 10 mm diameter sphere divided into four equally shaped sectors made of silver. The sectors are assembled on two superimposed printed circuit boards (PCBs). Each PCB provides mechanical support and signal routing, as shown in Fig. 1. A customized silicon die, manufactured in-house, with a deposited Pt resistor, is attached to each sector allowing temperature sensing and power injection. Two additional Pt resistors have been placed at the core of the sphere to mitigate and monitor heat conduction from the spherical sectors to the supporting structure.

In order to carry out the measurements presented in this paper, it is not necessary to have the sphere divided into sectors. The main advantage of this configuration is to use the probe also as a 3D heat flux sensor, as well as offering the possibility of exploring more complex measurements focused on the analysis of regolith inhomogeneity, which will be the objective of future work.

Fig. 2 shows a block diagram of the experimental setup and simplified schematic of the electronics used to measure the thermal impedance of the thermoprobe. An operational amplifier (OA) in inverting

* Corresponding author.
E-mail address: manuel.dominguez@upc.edu (M. Domínguez-Pumar).

https://doi.org/10.1016/j.sna.2022.114018
Received 31 May 2022; Received in revised form 17 October 2022; Accepted 15 November 2022
Available online 17 November 2022

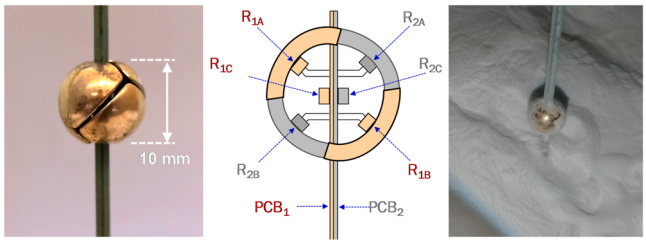

Fig. 1. (Left) Thermoprobe before filling the gaps between sectors. (Center) Diagrammatic cross-section of the thermoprobe showing the relative position of Pt sensors (Rxx) and the printed circuit boards (PCBx), (Right) Image showing the thermoprobe being deployed into a regolith simulant.

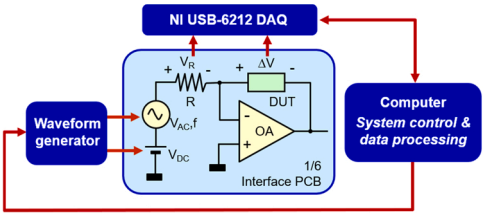

Fig. 2. Block diagram of the experimental setup and simplified schematic of the electronics used to measure the thermal impedance of the thermoprobe.

configuration is used to measure the impedance of each Pt resistor (DUT, device-under-test). The resistor R allows measurement of the injection of a sinusoidal current with bias into each DUT. By knowing the injected current and the voltage drop at each DUT, it is possible to obtain the value of each Pt resistor, and therefore its instantaneous temperature and injected power. Signals are monitored using a 16-bit ADC converter (NI USB-6212 acquisition system).

Fig. 3 shows the temperature and power signals in the Pt resistors in the sectors of the sphere and in the center of the sphere for a driving frequency of 3.973 mHz. a. Time evolution of the temperature in all four sectors (solid lines) and in the center of the sphere (dashed lines). b. Time evolution of temperature in sector 1 A. c. FFT of the absolute value of the temperature in sector 1 A: major contributions to the signal shown to be at the actuation frequency and at its second harmonic at double this frequency. d. and e. Time evolution of the applied power to sector 1 A and its FFT amplitude, respectively. For the power, the first three harmonics can be identified in the FFT. The thermal impedance at the actuation frequency is obtained as the quotient of the FFT temperature and the power signals at that frequency.

The core Pt resistors can be used to measure temperature and inject power at the center of the sphere. This capability is particularly important if using the structure as a wind sensor, [10,11]. In this case, the same current magnitude is applied in the cores as in the sectors. This way, the temperature evolution of the cores is similar to that of the sectors, as can be seen in Fig. 3.a, and heat transfer from the sectors to the supporting structure is mitigated. Additionally, before calculating the thermal impedance at each Pt resistor in the sector, an estimation of the heat transfer from the sector to the cores is obtained as: $P_{i-core} = \delta(T_i - T_{avg-cores})$, which represents the phasor of the heat transfer from sector i to the core of the sphere, and where $T_{avg-cores}$ is the average temperature phasor of both core resistors. Therefore, the thermal impedance of sector i, Z_i, is calculated as:

$$Z_i = \frac{T_i}{P_i - P_{i-core}} \tag{1}$$

Finally, the total measured impedance of the sphere, Z_{meas}, is obtained as the parallel impedance of the four sector impedances. The associated power transfer coefficient ($\delta = 0.4$ mW/K) was calculated in the fitting procedure explained in the next section.

3. Regolith characterization

Eight different regolith simulants made of hollow glass microbeads from SiLi® have been used to test the proposed measurement procedure. Each simulant was a mix of borosilicate glass microbeads of three different sizes, as specified in Table 1, together with other physical properties. The thermal conductivity and diffusivity reference values of the samples have been measured using the KD2 Pro Thermal Properties Analyzer operating with a dual-needle sensor (SH-1). The performance of the SH-1 was verified prior to measurements with the Delrin block provided by the manufacturer. The individual values of thermal

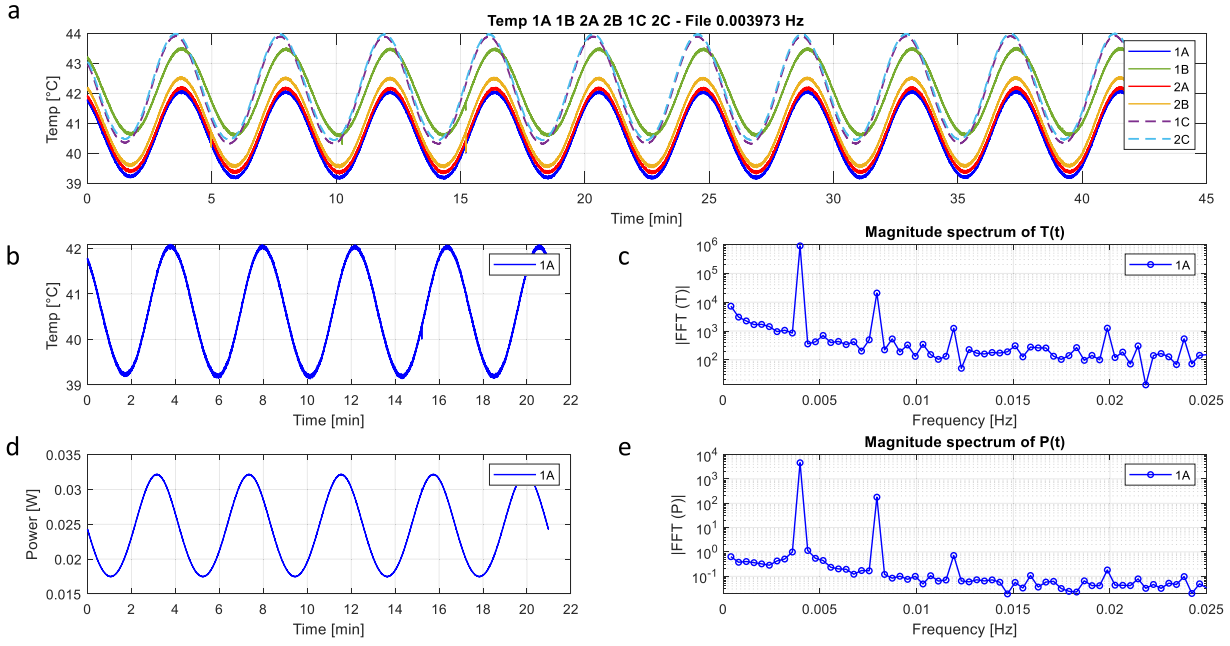

Fig. 3. Details of the measurement at frequency 3.973 mHz. (a) Temperature evolution at the Pt sector resistors (1A, 1B, 2A, 2B) and cores (1C, 2C). (b) Temperature evolution of sector 1A and its FFT amplitude (c). (d) Power signal applied to sector 1A and its FFT amplitude (e).

Table 1
Physical properties of the regolith samples and numerical values associated to the measurements of Fig. 7.

	Bulk	Particle	Crush	Thermal Conductivity			Thermal Diffusivity		
Sample	Density [g/cm³]	sizes [μm]	strength [MPa]	Reference [W/mK]	Measured [W/mK]	Error [%]	Reference [mm²/s]	Measured [mm²/s]	Error [%]
8015	0.10	30 / 70 / 90	2	0.0493	0.04851	-1.6	0.17178	0.16943	-1.4
8020	0.12	32 / 68 / 106	4	0.0467	0.04737	1.4	0.15901	0.14798	-6.9
8025	0.15	30 / 65 / 100	5	0.0520	0.05178	-0.4	0.15917	0.15971	0.3
8032	0.19	30 / 56 / 74	14	0.0510	0.05338	4.6	0.15804	0.15107	-4.4
8046	0.26	22 /45 / 65	41	0.0640	0.06377	-0.4	0.16068	0.15435	-3.9
8060	0.35	18 /40 / 60	55	0.0713	0.07574	6.2	0.15890	0.16291	2.5
8070	0.42	15 / 30 /40	124	0.0847	0.08196	-3.2	0.16081	0.15313	-4.8
8082	0.35	18 / 40 / 60	82	0.0723	0.07545	4.4	0.16056	0.16364	1.9

conductivity k_{DB}, volumetric specific heat capacity C_{DB} and diffusivity D_{DB} were compared to ones from the Certificate of Quality Assurance and did not deviate more than ± 3%. The device utilizes a transient line heat source with a dual probe analysis of the temperature vs time dependence. According to the equipment specifications, the expected accuracy is ± 5%. As it is mentioned in [14], the error analysis on the technique produces accuracy bounds depending on accuracy of the temperature measurements and positioning of the needles. The specifics of the measuring method and its error analysis may be found in [14,15].

Measurements were performed after a minimum 15 min of equilibration of the sensor after inserting it into the investigated specimen. The contact resistance, relatively higher in granular materials, was kept at a minimum level without using any additional thermal grease on the sensor. Due to the heat pulse generated by the sensor during the reading in order to achieve the best accuracy a layer of at least 2 cm of the investigated material was provided parallel to the sensor in all directions. The temperature of the sample was kept as constant as possible during the whole measurement. For each sample, 3 measurements were taken, and the time between individual readings was around 15 min. A default read time of two minutes was applied, during which 60 temperature records were taken. The direct values of thermal conductivity and thermal diffusivity are defined according to equations 8 and 10 of [15]. The mean values for specific regolith simulants are summarized in Table 1.

4. Experimental results

All eight regolith simulants have been measured with the spherical thermoprobe. The frequency ranged from approximately 1 mHz to 1 Hz. The number of signal periods per frequency was between 10 and 20 cycles. In the low frequency range, 10 cycles were used to avoid measurements longer than 24 h.

The total measured impedance of the thermoprobe, $Z_{meas}(\omega)$, was estimated as the parallel of the thermal impedances measured at the four Pt resistors of the sectors. To obtain the thermal conductivity, k_r, and diffusivity, D_r, of the regolith, a fitting procedure was used in which the measured value was modelled by the expected thermal impedance of a sphere placed in the regolith, in parallel with the thermal capacitance associated to the four sectors themselves. The heat capacitance associated to each sector was calculated taking into account the mass (0.431 g) and the heat capacitance of the alloy (93% Ag, 3.5% Cu, 3.5% Zn): 0.1059 J/K per sector. A contact resistance of 3.01 K/W was also calculated in the fitting procedure, as explained below.

According to [16, Section 3.6, page 121], the analytical expression of the Fourier transform of the thermal impedance of a sphere in a medium is:

$$Z_r[k,D](s) = \frac{1}{4\pi k r_0} \bullet \frac{1}{1 + r_0\sqrt{\frac{s}{D}}}, \tag{2}$$

where s is the Laplace complex variable, r_0 the sphere radius, k and D the thermal conductivity and thermal diffusivity of the medium, respectively.

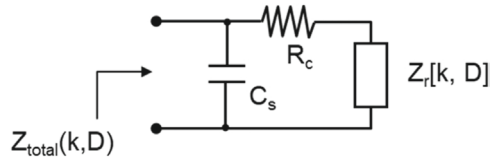

Fig. 4. Thermal model of the sphere. C_s corresponds to the capacitance of the sectors, R_c is the contact resistance between the sectors and the regolith, and Z_r is the thermal impedance of the regolith modelled by Eq. (2).

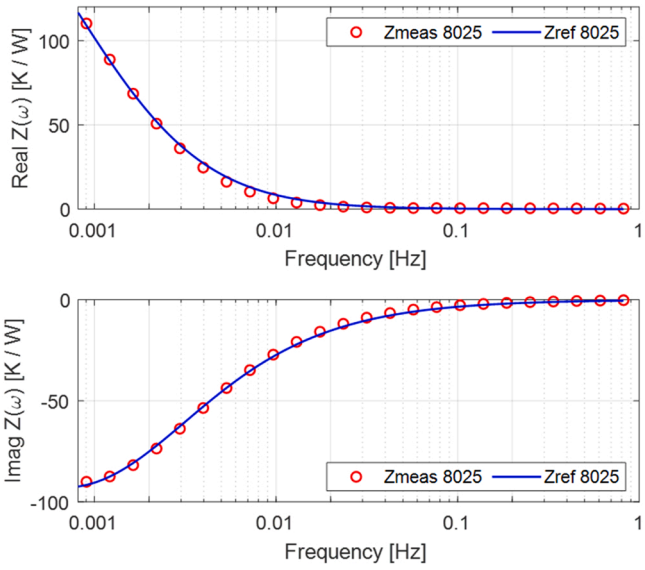

Fig. 5. Estimation of Real (top) and Imaginary (bottom) part of the thermal impedance of the thermoprobe obtained from the measurements with sample 8025 (red circles). The blue line has been obtained using the model and the reference values obtained in Section 3 for this regolith simulant.

Finally, the complete thermal model includes the thermal capacitance of the sectors and contact resistance between the sectors and the medium (regolith), is shown in Fig. 4.

The fitting procedure therefore finds the values k_r and D_r, as:

$$[k_r \quad D_r] = \underset{[k,D]}{\text{Argmin}}\left\{\sum_n |Z_{total}(k,D)(i2\pi f_n) - Z_{meas}(f_n)|^2\right\}, \tag{3}$$

where $f_n$is the set of frequency points used in the measurement. The power transfer coefficient δ and the contact resistance R_c were the common values of these parameters leading to minimum global error when comparing the estimated values of thermal conductivity and diffusivity with the reference values for the eight regolith simulants

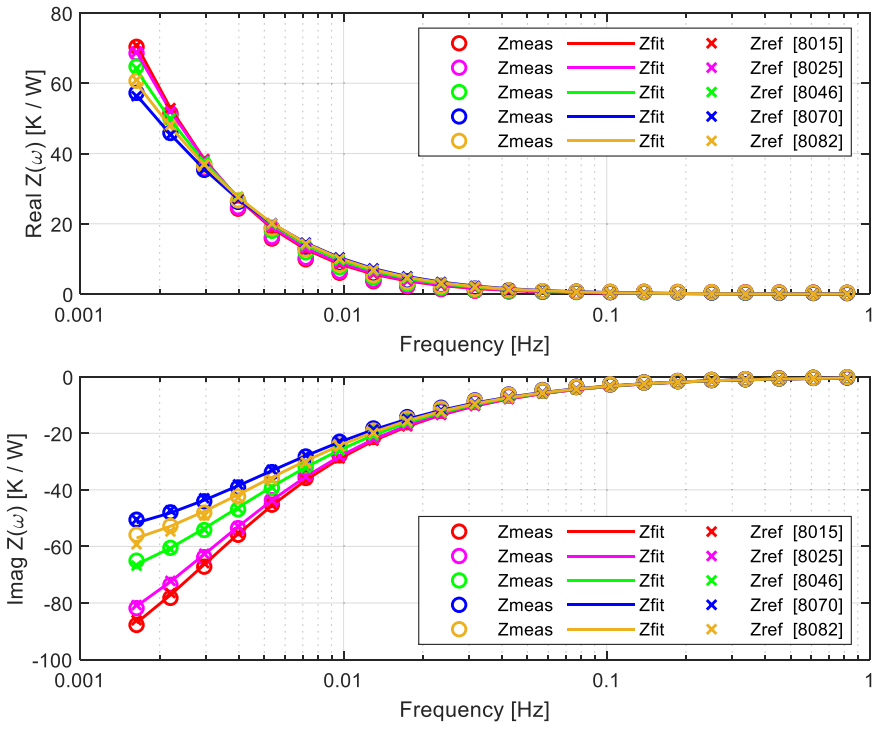

Fig. 6. Comparison between the measured thermal impedance of the thermoprobe (Z_{meas}, circles), the thermal model with the thermal conductivity and diffusivity values obtained from fittings using Eq. (3) (Z_{fit}, solid line), and the thermal model using the reference values for k_r and D_r (Z_{ref}, x symbols), for five regolith simulants.

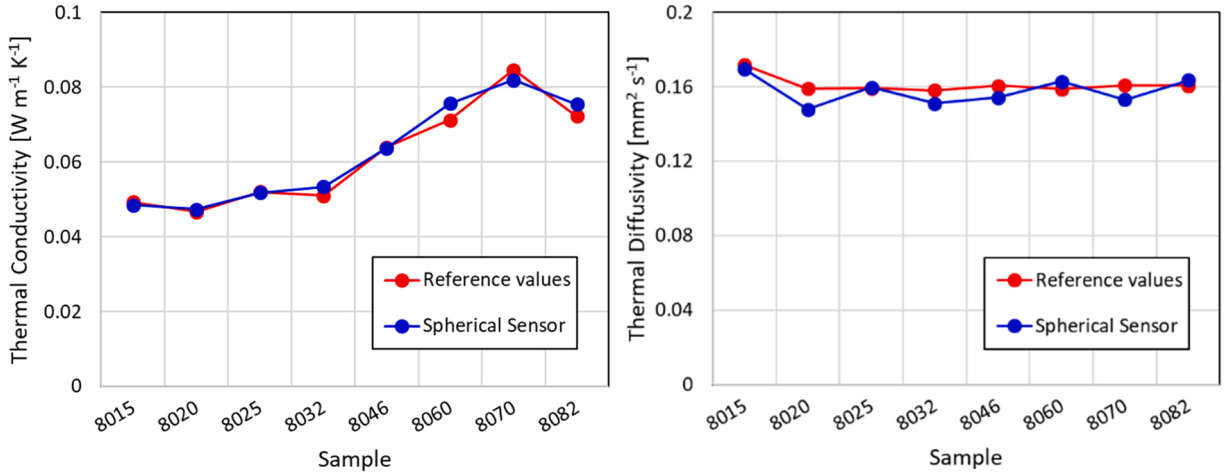

Fig. 7. Comparison between reference and measured values of the thermal conductivity (left) and diffusivity (right) for all simulant samples.

used.

Fig. 5 compares the thermal impedance seen from the Pt resistors with simulant 8025 obtained from the measurements (red circles) with its estimation using expression (2) above, including the parallel capacitance of the sectors and taking the reference values obtained in Section 3 for this regolith simulant (solid line). As can be observed, the experimental values clearly follow the trend predicted by the analytical model using the reference values.

Fig. 6 shows the estimation of the thermal impedances of five regolith simulants, as obtained from measurements (Z_{meas}, circles), superimposed with the analytical model and the estimated values obtained from fittings using Eq. (3) (Z_{fit}, solid line), as well as with the analytical model and the reference values (Z_{ref}, x symbols). As it can be observed, the impedances present different trends for different regoliths, and the fitted model and the measurement values are very close.

A comparison between reference and measured values of both the thermal conductivity and the diffusivity for eight different regolith simulants is shown in Fig. 7, while Table 1 reports the numerical values. As it can be seen, there is a good match between measured and reference values in all cases. The error is below ± 7% in both the thermal conductivity and the thermal diffusivity.

5. Conclusions

The results presented in this paper indicate that it is possible to extend the use of the spherical thermoprobe, beyond its capability of measuring 3D heat fluxes, to measure thermophysical properties of granular materials. By estimating the thermal impedance of the sphere in the frequency domain with the model used, it is possible to infer the thermal conductivity and diffusivity of regoliths. Experiments have been

carried out with eight different regolith simulants made of hollow glass microbeads, differing in density, crush strength and particle size. The results show that, for this set of regolith simulants, estimation errors are below ± 7% for both the thermal conductivity and diffusivity. Future work will be focused on analysing how the method works with multi-component regolith simulants and in the pressure conditions of the environment applicable to planetary bodies.

Funding

Funded in part by MICINN, grants no. RTI2018-098728-B-C33 and PID2021-126719OB-C42, and ESA contract 4000128070/19/NL/KML for the MiniPINS study.

CRediT authorship contribution statement

Conceptualization, M.D-P; Electronic system design, C.R-P, J.R-C, N. S-P, X.M; In-house sensor fabrication, J.P-N, V.J, M.D-P; Investigation, all authors; Regolith characterization D.S, A.J; Sensor measurements, C. R-P, M.D-P; Supervision, M.D-P; Writing – review & editing, M.D-P, J.P-N, D.S.

Declaration of Competing Interest

The authors declare that they have no known competing financial interests or personal relationships that could have appeared to influence the work reported in this paper.

Data Availability

Data will be made available on request.

References

[1] P.O. Hayne, J.L. Bandfield, M.A. Siegler, A.R. Vasavada, R.R. Ghent, J.P. Williams, D.A. Paige, Global regolith thermophysical properties of the moon from the diviner lunar, Radiom. Exp. J. Geophys. Res. Planets 122 (12) (2017) 2371–2400, https://doi.org/10.1002/2017JE005387.

[2] T. Zhang, B. Wang, H. Wei, Y. Zhang, C. Chao, K. Xu, Z. Zhao, Review on planetary regolith-sampling technology, Prog. Aerosp. Sci. 127 (2021), 100760, https://doi.org/10.1016/j.paerosci.2021.100760.

[3] T.G. Wasilewski, T. Barciński, M. Marchewka, Experimental investigations of thermal properties of icy lunar regolith and their influence on phase change interface movement, Planet. Space Sci. 200 (2021), 105197, https://doi.org/10.1016/j.pss.2021.105197.

[4] M.Ya Marov, A.V. Kolesnichenko, K.K. Manuilov, V.P. Osipov, The thermophob experiment: direct investigations of the thermophysical properties of the regolith of phobos, Sol. Syst. Res. 44 (5) (2010) 393–402, https://doi.org/10.1134/S0038094610050060.

[5] T. Zhang, C. Chao, Z. Yao, K. Xu, W. Zhang, X. Ding, H. Chen, The technology of lunar regolith environment construction on Earth, Acta Astronaut. 178 (2021) 216–232, https://doi.org/10.1016/j.actaastro.2020.08.039.

[6] R.M. Winglee, C. Truitt, R. Shibata, High velocity penetrators used a potential means for attaining core sample for airless solar system objects, Acta Astronaut. 137 (2017) 274–286, https://doi.org/10.1016/j.actaastro.2017.04.022.

[7] T. Spohn, T.L. Hudson, L. Witte, T. Wippermann, L. Wisniewski, B. Kedziora, J. Grygorczuk, The InSight-HP3 mole on Mars: lessons learned from attempts to penetrate to depth in the Martian soil, Adv. Space Res. 69 (8) (2022) 3140–3163, https://doi.org/10.1016/j.asr.2022.02.009.

[8] E.M. MacLennan, J.P. Emery, Thermophysical investigation of asteroid surfaces. I. Characterization of thermal inertia, Planet. Sci. J. 2 (4) (2021) 161, https://doi.org/10.3847/psj/ac1591.

[9] M. Domínguez-Pumar, J.A. Rodríguez-Manfredi, V. Jiménez, S. Bermejo, J. Pons-Nin, A miniaturized 3D heat flux sensor to characterize heat transfer in regolith of planets and small bodies, Sensors 20 (15) (2020) 4135, https://doi.org/10.3390/s20154135.

[10] L. Kowalski, M.T. Atienza, S. Gorreta, V. Jiménez, M. Domínguez-Pumar, S. Silvestre, L.M. Castañer, Spherical wind sensor for the atmosphere of Mars, IEEE Sens. J. 16 (7) (2015) 1887–1897, https://doi.org/10.1109/JSEN.2015.2509168.

[11] M. Domínguez-Pumar, L. Kowalski, V. Jiménez, I. Rodríguez, M. Soria, S. Bermejo, J. Pons-Nin, Analyzing the performance of a miniature 3D wind sensor for Mars, Sensors 20 (20) (2020) 5912, https://doi.org/10.3390/s20205912.

[12] O. Carpentier, D. Defer, E. Antczak, T. Chartier, Frequency methods applied to the characterization of the thermophysical properties of a granular material with a cylindrical probe, Int. J. Thermophys. 33 (1) (2012) 105–120, https://doi.org/10.1007/s10765-011-1112-x.

[13] C. Dames, G. Chen, 1ω, 2ω, and 3ω methods for measurements of thermal properties, Rev. Sci. Instrum. 76 (12) (2005), 124902, https://doi.org/10.1063/1.2130718.

[14] G.J. Kluitenberg, J.M. Ham, K.L. Bristow, Error analysis of the heat pulse method for measuring soil volumetric heat capacity, Soil Sci. Soc. Am. J. 57 (6) (1993) 1444, https://doi.org/10.2136/sssaj1993.03615995005700060008x.

[15] K.L. Bristow, G.J. Kluitenberg, R. Horton, Measurement of soil thermal properties with a dual-probe heat-pulse technique, Soil Sci. Soc. Am. J. 58 (5) (1994) 1288, https://doi.org/10.2136/sssaj1994.03615995005800050002x.

[16] D. Maillet, S. André, J.C. Batsale, A. Degiovanni, C. Moyne, Thermal Quadrupoles: Solving the Heat Equation through Integral Transform, John Wiley & Sons, 2000.

Manuel Domínguez-Pumar obtained his MSc and PhD degrees in Electronic Engineering both from the Universitat Politecnica de Catalunya (UPC), Spain, in 1994 and 1997, respectively. He is Full Professor at the UPC. He leads the Mars Lab, within the Micro and Nanotechnologies group at UPC. He has participated in the development of wind sensors for instruments on three NASA missions: REMS (Mars Science Laboratory), TWINS (InSight) and MEDA (Mars2020). He obtained a NASA group award. Presently, he is Co-Investigator in European Space Agency's Contract, titled Miniaturized Sensor Packages and Delivery Systems for In-Situ Exploration. He has published more than 70 journal papers.

Carlos Rosero-Pozo, received the BSc degree in Electronic Engineering from the Escuela Politécnica Nacional (EPN), Quito, Ecuador, in 2018. Subsequently, he joined to the Physics Department, EPN, as a teaching assistant until 2020. From 2016–2020, he was a research assistant with the Astroparticles Laboratory, EPN, involved on the design of water Cherenkov detectors. Since 2021, he is a PhD candidate in the Electronic Engineering Department, Universitat Politècnica de Catalunya (UPC), Barcelona, Spain. He is working on the design and test of sensors for planetary bodies

Joan Pons-Nin is an Associate Professor with the Department of Electronic Engineering at the Telecommunications Engineering School of Barcelona, Spain. He received the MSc (1989) and PhD (1995) degrees in Electronic Engineering from the Universitat Politècnica de Catalunya (UPC). He has worked on oscillators for MEMS and non-linear dielectric charge control systems applied to MEMS, MOS and perovskite-based devices. He is currently working on wind, heat flux and magnetic sensors for space. He has authored 41 papers in scientific journals and 63 congress communications.

Juan Ramos received the Telecommunication Engineering and PhD degrees from the Universitat Politècnica de Catalunya (UPC), Barcelona, Spain, in 1992 and 1997, respectively. He is Associate Professor at the Electronic Engineering department of UPC, teaching courses in several areas of electronic instrumentation. His research areas of interest are on the design of ultra-low noise measurement systems with applications into the biomedical and space instrumentation fields. He participated in the LISA PathFinder since 2004, and since 2019 he is working on the development of the diagnostics subsystem of the LISA mission. He is co-IP of the IEEC group that develops high computing performance multi-purpose Nanosat platforms.

Daria Szewczyk received her Engineer and MSc degree from Wroclaw University of Science and Technology in 2011 and 2012, respectively. She completed her PhD studies with honors in Physical Sciences at the Institute of Low Temperature and Structure Research of Polish Academy of Sciences in Wrocław in 2019, where she is now an Associate Professor at the Department of Low Temperature and Superconductivity. Her field of work is focused on advanced thermal transport investigations of a wide variety of different systems like molecular crystals exhibiting disorder, glassy type materials, carbonbased nanomaterials, manganites and hybrid perovskites.

Andrzej Jeżowski received his PhD at the Institute of Low Temperature and Structure Research of Polish Academy of Sciences in Wrocław in 1983. In 1998 he obtained a Professor title from the President of Poland. For many years he was the head of the Laboratory of Cryocrystals and the Head of the Division of Low Temperature and Superconductivity at ILT&SR PAS. Since 2011 he is the Director of the Institute. He is a recognized expert in the field of thermal transport physics with over 220 publications. He was a PI of many bilateral collaborations and grants. He is a member of the Scientific Councils of other Institutes.

Nil Solà-Peñafiel received the Telecommunication Engineering degree from the Universitat Politècnica de Catalunya (UPC), Barcelona, Spain, in 2021. He is currently a research assistant at the Micro and Nano Technologies group, Electronic Engineering department of UPC. His research interests include sensors for space application, closed-loop control systems, sigma-delta modulators, and MEMS sensors and actuators.

Xavier Manyosa received the Telecommunication Engineering degree from the Universitat Politècnica de Catalunya (UPC), Barcelona, Spain, in 2021. He is currently a research assistant at the Institute of Space Sciences of Catalonia (IEEC). His research interests include magnetic field sensors, smart control and interface electronics for sensors and MEMS, for space-related applications.

Sandra Bermejo Broto received the MSc in Electrical Engineering and the PhD degree in 2000 and 2004 respectively. She is currently leading the electro-kinetics research in the Electronic Engineering Department at UPC. Her work is aimed to develop approaches tailored towards the fabrication of functional nano-devices by electrowetting and electrospray techniques in the fields of photonics, energy and sensing. She has been

responsible of the fabrication of the first energy harvester's super-capacitor fully developed with dielectric nanoparticles. She is author of more than 40 international journal papers and book chapters and more than 40 international conference papers.

Vicente Jiménez Serres is a Telecommunications Engineer (E.T.S. de Ingeniería de Telecomunicación de Barcelona, 1992) and Doctor in Telecommunications Engineering (Technical University of Catalonia - UPC, 1997). Since 1998 he is an Associate Professor with the Electronics Engineering Department of the UPC. Most relevant recent scientific work has been developed in thermal anemometry for the REMS and MEDA instruments developed for the last two NASA Mars rovers. He has authored more than 40 scientific papers in international journals and conferences and supervised 2 PhD theses.